JOURNAL OF NEUROPHYSIOLOGY
Vol. 41, No. 3, May 1978. *Printed in U.S.A.*

Effect of Load Disturbances During Centrally Initiated Movements

E. BIZZI, P. DEV, P. MORASSO, AND A. POLIT

Department of Psychology, Massachusetts Institute of Technology, Cambridge, Massachusetts 02139

SUMMARY AND CONCLUSIONS

1. We have investigated the relative contributions of mechanical and reflex mechanisms in generating the forces produced by the neck muscles when loads were unexpectedly applied during centrally programmed head movements in monkeys. These movements, subserved by muscles well endowed with muscle spindles, are part of the coordinated eye-head response to the appearance of a stimulus in the animal's visual field. Our preparation was a chronically vestibulectomized monkey trained to make a visual discrimination.

2. Two procedures were used to evaluate the torque generated by the neck musculature when an unexpected load disturbance was applied: first, by surgically interrupting the afferent loop subserving the reflex action (section of cervical dorsal roots) and second, by building a mathematical model of the head-neck system and carrying out a process of simulation.

3. Our results indicated that the compensatory torque of reflex origin stimulated by the application of an opposing force was less than 10–30% of that required for perfect compensation, and the larger fraction of the observed compensation was due to the mechanical properties (inertial, viscous, and elastic) of the neck musculature. The combined action of reflex and mechanical processes never completely compensated for the disturbance.

INTRODUCTION

How effectively do primates compensate when their movements are met by unexpected load disturbances? To this deceptively simple question one cannot give an equally simple answer. In fact, a number of processes of great complexity, some only barely understood, are put into action by the sudden application of a load opposing a centrally initiated movement. To begin to unravel such complexities it is important to consider first the basic fact that load disturbances are resisted initially by two mechanisms: *1*) purely mechanical action of the activated muscle tissue, and *2*) reflex action. Both mechanisms generate a force opposing the increased load but the relative contribution of the reflex and mechanical actions are not yet known and may vary depending on the state of muscular activity and magnitude of load disturbance.

Although it is well known that the elasticity of activated muscle resists loads, the resistance generated by the reflex response to the load changes depends on a number of factors. Among these, perhaps the most relevant is the existence of alpha-gamma coactivation during centrally programmed movements. This coactivation has been observed by many investigators in a number of systems (12, 17, 19, 25, 35–39); for instance, the experiments by Severin et al. (35) have shown that during locomotion, reflex activity from IA afferents is greater from the shortening agonist muscle than it is from the lengthening antagonists. Results such as these indicate that gamma impulses are sent to the muscle spindles just prior to, or during, extrafusal contraction to induce intrafusal muscle contraction, which results in an increased group IA afferent activity. It has been suggested that through this coactivation of alpha and gamma elements, a mobile part of the body is "servo assisted" so as to adjust its force output to compensate for changes in load (25–27). However, to properly evaluate the complexities underlying load compensation, it is important to consider some of the interacting processes that occur at spinal and supraspinal levels following the application of a load. Among these, it is relevant that alpha motoneurons receive not only facilitation from muscle spindle afferents, but also an inhibitory input from Golgi tendon organs. In addition, afferent proprioceptive impulses reach subcortical and cortical areas (3, 7, 9, 15, 23, 28, 31, 32, 40, 41), generating corticofugal impulses that play back on the segmental apparatus, and these long loop reflexes

Received for publication May 16, 1977.

0022-3077/78/0000-0000$01.25

may be influenced by preexisting sets or instructions (16). These few examples suggest an exceedingly complex situation characterized by parallel processing along various segmental and suprasegmental pathways. Accordingly, the extent to which movement may be servo assisted (27) needs to be evaluated on its own merit, aside from the question of coactivation as such.

In the experiments to be reported here we have investigated the relative contributions made by the reflex and mechanical mechanisms to the increased force produced by the neck muscles when loads were unexpectedly applied during centrally programmed head movements in monkeys. These movements, subserved by muscles well endowed with muscle spindles (10), are part of the coordinated eye-head response to the appearance of a stimulus in the animal's visual field (4, 5).

We have approached the problem of evaluating the increment of reflex and mechanical torque generated by the animal by comparing head movements before and after surgical interruption of the afferent pathway subserving the reflex underlying the hypothesized servo action (section of cervical dorsal roots). Our results indicate that the compensatory torque of reflex (segmental and/or suprasegmental) origin, stimulated by the application of an opposing force, was from 10 to 30% of that required for perfect compensation, and that the larger fraction of the observed compensation was due to the mechanical (inertial, viscous, and elastic) properties of the neck musculature. Further, the combined action of reflex and mechanical processes never completely compensated for the disturbance.

METHODS

Procedure to elicit visually triggered eye-head movements

Three adult chronically vestibulectomized monkeys (*Macaca mulatta*) were trained prior to surgery to make a visual discrimination between a horizontal and a vertical bar (3′ of arc in width). The animals were reinforced with drops of water if they pressed a lever when the vertical bar appeared.

A PDP-11 computer was programmed to provide automatic presentation of the target light, which elicited the coordinated eye-head movements. The lights were placed in a horizontal perimeter arc 60 cm from the animal and were spaced at intervals of 10° of visual angle along the arc, ranging from 40° left of the midsagittal plane to 40° to the right of it. To generate sets of movements with uniform starting positions, the first part of the sequence (blank light) appeared directly in front of the animal at the center of the perimeter arc, with the result of attracting the animal's gaze to it. The blank light at the center was then turned off while the sequence containing the horizontal-vertical bars or the vertical bar alone appeared at some other position in the arc. In this way it was possible to collect sets of rather uniform eye-head movements starting from the center of the arc and directed to targets at 30 and 40° on either side. Although the animals could make the discrimination between the horizontal and vertical bar by moving only their eyes, they consistently chose to make the coordinated eye-head movement toward the light. The schematic Fig. 1 indicates the sequence of events during a trial.

Recording of head movements

Screws were permanently implanted in the skull to be used as connectors to the head holder (14). A lightweight apparatus (moment of inertia was 670 g · cm^2), which restricted head movements to the horizontal plane, was attached to the head screws and used to monitor these movements by means of a low-torque potentiometer connected to the shaft of the head holder. The shaft of the head holder could be suddenly and unexpectedly coupled with a specially designed

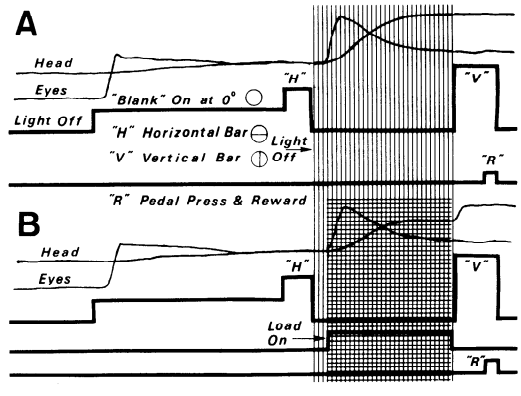

FIG. 1 Sequence of events during a trial. *A* shows the sequence for an unloaded movement starting at 0°. The first event is the target light onset at 0°, followed by a light with a thin horizontal bar appearing at some other position. The light is then switched off within the reaction time of the monkey but after the monkey has programmed an eye and head movement to the target. After a random delay the target light reappears with either a horizontal or vertical bar. The monkey must press a foot pedal during the appearance of the vertical bar to obtain a reward. The sequence of target-light presentation was randomized so that either the horizontal or vertical bar appeared first at the target location. The duration of each light was also randomized. *B* indicates the sequence of events during a loaded trial. The main difference between *A* and *B* is that a mechanical load is applied to the head during the interval in which the target light was switched off. The load was switched off before onset of the light and loads were applied on 5–10% of trials.

spring which applied a constant torque disturbance during the head movement. The load was monitored by a strain gauge. The application of the load generated a small click which was not detected by the monkey because the vestibulectomy impaired the monkey's auditory functions. A control experiment in which the click was delivered during the movement without concomitant load application generated no change in head trajectory. Load application was triggered by the appearance of EMG activity in the agonist muscle. (Peak head torque produced by the animal for a 30° movement is approximately 1,000 g · cm or 0.098 Newton · meter (Nm).)

Surgical interventions

Because our aim was to study the role of neck proprioceptors during head movements, we eliminated other sources of afferent input such as vestibular, and those from the periosteum surrounding the screws in the skull. We performed a bilateral labyrinthectomy 3 mo prior to the actual experimental sessions. This operation was performed under Nembutal anesthesia by drilling through the mastoid, exposing and opening the canals and filling them with dental cement. The effectiveness of the labyrinthectomy was tested by repeatedly rotating the animals in the dark to determine that nystagmus was absent. Chronically vestibulectomized monkeys recover their ability to perform very effective visually triggered eye-head movements (13).

The periosteum was surgically removed from around the screws implanted in the skull so that a force applied to the screws (to load the head during movement) would not be sensed at the point of entry of the screws into the skull. As an extra precaution, a local anesthetic was injected at these stress points prior to each experimental session. It should be noted that during load application in the rhizotomized animal, no change in EMG was observed. This indicates a satisfactory elimination of any reflex in response to perturbation of the body. Large torques, in excess of those normally generated by the animal, were applied only infrequently.

Cervical rhizotomy (C_1–T_3) was accomplished under a dissecting microscope with sparing of small vessels intermingled with dorsal rootlets. The dorsal roots were reached by first separating the neck muscles from the spinous processes and then removing the laminae with a rongeur. The dura was opened in the midline along the entire length of the laminectomy. After dorsal root section, the dura was sutured so that it was watertight. The wound was closed in layers.

Recovery of head movement

Rhizotomized, chronically vestibulectomized monkeys hardly moved their heads during the first postoperative week. After 8–10 days, they progressively recovered eye-head coordination, and by 15–20 days, fully developed head movements were observed. From this time on, no significant change in averaged peak acceleration was observed in all three monkeys. No retesting or training was done during this period of time. Regular experimental sessions were resumed after the 3rd wk.

Completeness of dorsal root section

Functionally, the completeness of dorsal root section was indicated by the absence of any short-latency response in the EMG following an externally imposed sudden head displacement in complete darkness. In addition, unexpected application of loads during centrally initiated head movements were not followed by an increase in EMG activity. Since afferents occur in ventral roots (8) and because of the impossibility of sampling all motor units in all the neck muscles for short-latency stretch responses, this test is not an entirely conclusive indicator of deafferentation. Anatomically, the dorsal root section was found to be complete by examining stained serial spinal cord sections. EMG activity was recorded by way of wires (100 μm) chronically implanted in right and left splenii capitis.

Data analysis

Data (head position, force) recorded on an FM tape recorder were sampled by a PDP-11 computer every 3 ms per channel and converted to physical units (degrees, Nm). Velocity and acceleration were obtained by numerical differentiation. For each individual record of head position, the instant at which the velocity exceeded a preset arbitrary value was used as the origin of the time axis for the purpose of alignment. The movement curves were subsequently averaged and the standard deviation was computed.

Derivation of head-neck model and estimation of passive and active parameters of neck musculature

In order to assess the relative contribution to load compensation of the viscoelastic properties of the system and of neural feedback, we developed a model of the mechanical properties of the head-neck system and simulated it on the computer. Basically, the model we have used contains the following: *1*) components with inertial viscous, and elastic characteristics representing the corresponding characteristics of head and neck tissue; and *2*) a torque-generating system, i.e., the activated musculature which, on receiving an input, moves the load. Those components whose values were not dependent on the level of neural input were termed "passive." Those components of muscle stiffness and

viscosity (defined later) which did depend on neural input were termed "active." In generating the model, the simplifying assumption was made that all elements contributing viscous and elastic loads are "lumped," acting between a stable platform, the shoulder girdle and the spine, and the moving element, the skull. Disturbances, i.e., external sources of torque, could also be applied to the system (Fig. 2). In the following paragraphs we indicate the conceptual basis of both the experiments and the computation required to estimate the value of the parameters.

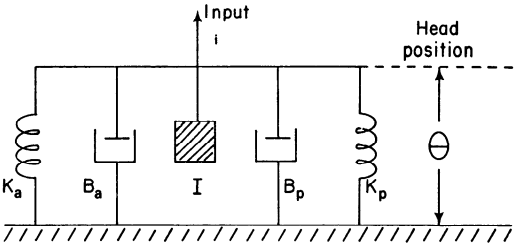

FIG. 2. A model representing the mechanical properties of the head-neck system. Tissues and joints contribute viscoelastic properties represented by springs and dashpots. The head also has a moment of inertia, I. The effect of neural input to muscles is represented by a torque-generator, i. Externally applied torque disturbances are applied at the same location as i. K and B are coefficients of passive elasticity and viscosity, whereas K_a and B_a are their active counterparts.

Computation of inertial resistance

The mass of the bone and soft tissue, rotating about a vertical axis, possesses a moment of inertia that requires torque for acceleration or deceleration. Since body movement was found to be insignificant, it could be safely assumed that, for each head-turning movement, the head rotated about an axis that remained fixed in space.

The moment of inertia, I, was computed by applying a pulse of torque ($L_{applied}$) to the severed perfused head (together with neck muscles) while it was connected to the head holder; in this case, its angular acceleration, $\ddot{\theta}$, depended solely on its moment of inertia. The friction of the head holder (L_{fric}) eventually brought the head to rest. The rotation of the head obeys the following equations:

$$L_{applied} + L_{fric} = I\ddot{\theta}$$

during the application of the torque pulse, and

$$L_{fric} = I\ddot{\theta}$$

following the termination of the torque pulse. For the purpose of computation of moment of inertia, only those segments of the head-position record were used in which the acceleration and deceleration of the head were observed to be constant. This procedure simplified the computation because, during these periods, both frictional and applied forces are constant. The applied torque was known and the angular acceleration was measured. Thus the equations could be solved and the moment of inertia, I, obtained. The method actually used involved simulating the equations on the computer and varying the parameter I until the simulated head movement most closely resembled the actual data, the criterion being the minimization of the mean square error. Since a constant value for the parameter I was sufficient to produce a good fit (root mean square error less than 1°), it was assumed that the moment of inertia remained constant during a head movement (Table 1). Any contribution of the vertebral column to the total moment of inertia can be expected to be small because of the small diameter of the structure compared to that of the skull. The moment of inertia of the head-holding apparatus was 5% of the total moment of inertia.

Computation of elastic restoring force

In order to measure the passive elastic forces, we minimized both the spontaneous and the reflex input to the neck muscles by using an anesthetized and rhizotomized animal, seated upright in the chair and fitted with the head-holding apparatus. Under these conditions, the head returns to the primary position, i.e., facing straight ahead, when released from any other position. The torque needed to hold the head in a deflected position increased with deflection, indicating a force that can be modeled as an elastic restoring force. Torque loads of different magnitudes were applied and the resulting deflections were plotted on a graph of applied torque versus head deflection. Typical loads for one monkey ranged from 0.037 to 0.12 Nm, with head deflections ranging from 4 to 30°. A straight line was fitted to the points using the minimization of mean square error as a criterion and the slope of the straight line provided the value of the coefficient of elasticity. It should be noted that, for small applied torques, the deflection was substantially smaller than predicted by the straight-line fit, indicating a high stiffness. Consequently, for the purpose of this model we relied on data taken from larger deviations, and the coefficient of elasticity was assumed to be a constant, K_p (Table 1). In this paper, we define stiffness (K_p), i.e., the coefficient of elasticity, as the slope of the measured torque-deflection curve.

Computation of viscosity

A major source of resistance exerted by the passive tissue, including muscle, is assumed to be

TABLE 1. *Values of mechanical parameters*

Experimental Preparation	Mechanical Parameters	Monkey *43*	Monkey *50*	Monkey *54*	Units
Head only	I	0.002	0.0018	0.0025	Kg·m²
Deafferented vestibulectomized anesthetized	B_p*	0.005–0.085	0.007–0.027	0.01–0.03	Nm s/rad
	K_p	0.1	0.105	0.15	Nm/rad
Deafferented vestibulectomized	B_a†	0.005 (0.005–0.008)	0.005 (0.0–0.01)	0.005 (0.005–0.007)	Nm s/rad
	K_a†	0.2 (0.1–1.0)	0.15 (0.0–0.25)	0.35 (0.1–0.8)	Nm/rad
Vestibulectomized (proprioception intact)	B_a†	0.005 (0.005–0.01)	0.005 (0.0–0.015)	0.005 (0.005–0.007)	Nm s/rad
	K_a†	0.25 (0.1–0.7)	0.18 (0.0–0.4)	0.35 (0.1–1.2)	Nm/rad

Abbreviations for units: kg·m², kilogram·meter·meter; Nm s/rad, Newton-meter·second/radian; Nm/rad, Newton-meter/radian. * Viscosity of passive tissue was found to have a nonlinear dependence on head velocity and acceleration. The range of values presented indicates the change in viscosity estimated to occur during a movement. † Stiffness and viscosity of activated muscle was observed to be dependent on the level of activation, as determined by electromyographic activity. The most frequently observed value and the range of observed values are presented. The most frequently observed values of K_a and B_a, obtained for the deafferented animal, were the ones used in the model when evaluating the mechanical and neural components of torque developed in response to disturbance during a movement.

viscosity, i.e., a retarding force that increases as the angular velocity of the head increases. Derivation of the coefficient of viscosity was based on the application of steps of torque to the anesthetized, rhizotomized monkey. Since the applied torque was known, and the moment of inertia and the coefficient of elasticity had been derived, the coefficient of viscosity (B_p) was obtained by simulating and solving the following equation of motion:

$$L_{applied} = I\ddot{\theta} + B_p\dot{\theta} + K_p\theta$$

The head position and its angular velocity and acceleration, θ, $\dot{\theta}$, and $\ddot{\theta}$, respectively, were measured. The term L_{fric}, the frictional force of the apparatus, does not appear in this and subsequent equations because it was found to be negligibly small ($L_{fric} = 0.007$ Nm).

Since a constant value of the coefficient of viscosity was found not to produce a good fit, we have represented the coefficient of viscosity, B_p, measured in the anesthetized animal, as a quantity whose value decreases when either the velocity or the acceleration increases (Table 1). This representation of the coefficient of viscosity yielded a good fit for deflections generated by the step application of torques ranging from 0.04 to 0.12 Nm.

Length-tension properties

We derived the length-tension properties of the active head-neck system by a method similar to that used for the coefficient of elasticity of passive tissue. Step torque disturbances of different magnitudes (0.4–0.12 Nm), applied to the head of the awake, chronically vestibulectomized and rhizotomized animal when it was fixating a target, produced deflections (2–17°) which depend on the stiffness of both passive tissue and active muscle. (Note that the fixating light was turned off during load application, thus leaving the animal in darkness.) In the rhizotomized animal, the disturbance did not alter the motoneuron output that maintained the original fixation. Thus neural input to both agonist and antagonist muscles remained constant, and the disturbance was used to measure the combined length-tension properties of both groups of muscles. The slope of the length-tension curve represents the coefficient of elasticity of the entire head-neck system, i.e., stiffness of passive tissue (K_p) and active muscle (K_a), and was computed as the slope of the straight line that best fit the observed data of applied torque versus observed deflection. Under the assumption that the length-dependent properties of active muscle can be represented by an elastic element which acts to increase the stiffness of the total system, subtracting the coefficient of elasticity of passive tissue (K_p) from the total measured coefficient of elasticity leaves the coefficient of elasticity of active muscle (K_a).

The range of values of the coefficient of elasticity obtained for each monkey are indicated

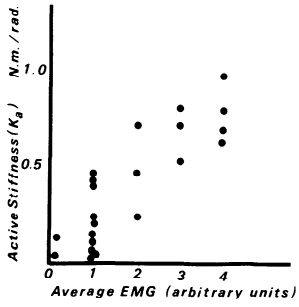

FIG. 3. Relationship between average level of EMG activity and measured active muscle stiffness during posture in one animal. High levels of EMG activity could be observed in all head positions, but occurred primarily when the head was held deviated from the forward-facing position.

in Table 1. It is to be expected that the muscle stiffness will vary with increasing neural input to the muscles, and this might explain the range of observed values (1, 2, 20, 33). In our own measurements of muscle stiffness, the relationship is as shown in Fig. 3. We made the measurement of stiffness 3–4 wk after deafferentation, i.e., when recovery from surgical intervention was well underway. The rationale for using the rhizotomized animal to measure active stiffness was to avoid contamination of the measured deflection by the reflexly induced opposing forces. It should be noted that the values of stiffness found by applying the same procedure to the vestibulectomized but otherwise intact animal were not significantly different from those found in the deafferented preparation (see Table 1 and Fig. 4).

Force-velocity properties

When the animal is awake, the neural input to the muscles causes a small increase in the viscosity, which is represented by B_a, the coefficient of viscosity of the activated muscle. The total viscous drag is represented by the expression $(B_p + B_a)\dot{\theta}$, where $\dot{\theta}$ is the angular velocity of the head. To evaluate the parameter, B_a, we applied step disturbances to the awake, rhizotomized animal fixating a target and the resulting head movement was fitted by the following equation:

$$L_{applied} = I\ddot{\theta} + (B_p + B_a)\dot{\theta} + (K_p + K_a)\theta$$

for a target at 0°. The range of velocities achieved during load application encompassed those occurring during natural head movements. The value of B_a, the coefficient of viscosity for active muscle, was varied until a good fit was obtained using the minimization of mean square error as a criterion (root mean square error less than 2°). A similar fitting procedure was used for targets at other locations with similar results. The value of B_a was found to be small (Table 1) and no firm evidence could be obtained for its dependence on head position or velocity.

Representation of input

The input to the model is a time-varying function, i(t). This function, i, can be thought of as a symbolic representation of alpha motoneuron activity to the total neck musculature. The mathematical representation of the input is:

$$i(t) = I\ddot{\theta} + (B_p + B_a(t))\dot{\theta} + (K_p + K_a(t))\theta$$

or, for simplicity,

$$i = I\ddot{\theta} + (B_p + B_a)\dot{\theta} + (K_p + K_a)\theta \qquad (1)$$

where I is the moment of inertia, B_p is passive viscosity, $B_a(t)$ is active viscosity, K_p is passive stiffness, $K_a(t)$ is active stiffness, $\ddot{\theta}$ is head angular acceleration, $\dot{\theta}$ is velocity, θ is position, and t is time. Though $B_a(t)$ and $K_a(t)$ presumably change in time as a result of changing neural input, only the most frequently observed values of B_a and K_a were used in the model when simulating a movement. By taking into consideration the fact that the torque developed by the input, i, to the model is used to overcome passive elastic $(K_p\theta)$, viscous $(B_p\dot{\theta})$ and inertial resistances $(I\ddot{\theta})$, we can rewrite *equation 1* as:

$$i = (I\ddot{\theta} + B_p\dot{\theta} + K_p\theta) + B_a\dot{\theta} + K_a\theta \qquad (2)$$

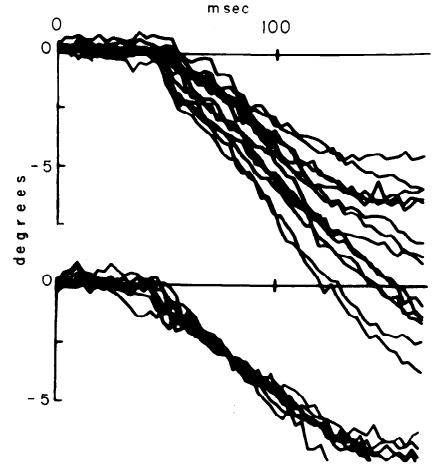

FIG. 4. Trajectories of head deflection during application of a step torque of 0.07 Nm (upper figure, intact animal; lower figure, deafferented animal). The similarity in the early portion (first 50 ms) of trajectories of the intact and deafferented animals indicates that deafferentation has not altered the inertial and viscous properties of the neck musculature. The spread in the later portion of the trajectories of the intact animal indicates the observed range of values of muscle stiffness. This range encompasses values of muscle stiffness observed in the deafferented animal.

or

$$i = T + B_a\dot{\theta} + K_a\theta \quad (3)$$

where

$$T = I\ddot{\theta} + B_p\dot{\theta} + K_p\theta \quad (4)$$

We can further rewrite *equation 3* as

$$T = i - B_a\dot{\theta} - K_a\theta \quad (5)$$

We interpret T as the torque developed by the muscles in response to neural input. *Equation 5* indicates that this torque is a function of neural input as well as of muscle length and rate of change of length (length-tension and force-velocity properties of muscle). *Equation 4* indicates that this torque is utilized to overcome the passive resistances to movement. When an external opposing load is present, *equation 1* is modified to become

$$i = I\ddot{\theta} + (B_p + B_a)\dot{\theta} + (K_p + K_a)\theta + L \quad (6)$$

Utilizing model

With the estimation of the parameters K_p, K_a, B_p, B_a, and I, the model is completely specified. It can now be used in two modes:

MODE 1. For any movement generated by the monkey, θ, $\dot{\theta}$, and $\ddot{\theta}$ can be measured (sampled at intervals during the movement) and the corresponding time-varying input, i, or torque, T, can be computed by using the *equations 1* and *4*, where all the terms on the right-hand side of the equation are known.

MODE 2. For any time-varying input, i (such as the result of the computation above), the resulting head movement, θ, can be computed using *equation 1* again. In this case, it is the term on the left-hand side of the equation that is known.

In both cases, disturbances can be applied to the model to simulate the application of loads to the monkey's head, as is indicated in *equation 6*.

RESULTS

Basic preparation and procedure

As mentioned earlier, the application of a load disturbance during head movement is resisted by the intrinsic stiffness of the activated muscle tissue and by the increased alpha motoneuronal activity evoked by reflex proprioceptive mechanisms. Because our aim was to evaluate the relative contribution of neck proprioceptors during load applications, we eliminated other sources of afferent input such as vestibular, visual, and the afferents from the periosteum surrounding the screws in the skull. Under these conditions only the neck proprioceptive apparatus could convey information about external load disturbances applied to the head and contribute to its compensation. The excitation of this apparatus by application of an external force reliably elicited short-latency electromyographic changes in stretched neck muscles within 20 ms; predictably, this response disappeared after bilateral C_1–T_2 dorsal roots section.

Contribution of reflex activity to load compensation: deafferentation experiments

APPLICATION OF FORCE DISTURBANCES DURING HEAD MOVEMENTS IN CHRONICALLY VESTIBULECTOMIZED ANIMALS WITH INTACT DORSAL ROOTS. Short-latency reflex increases in electromyographic activity were easily observed not only when a force disturbance was applied during postural stabilization, but also during visually evoked head

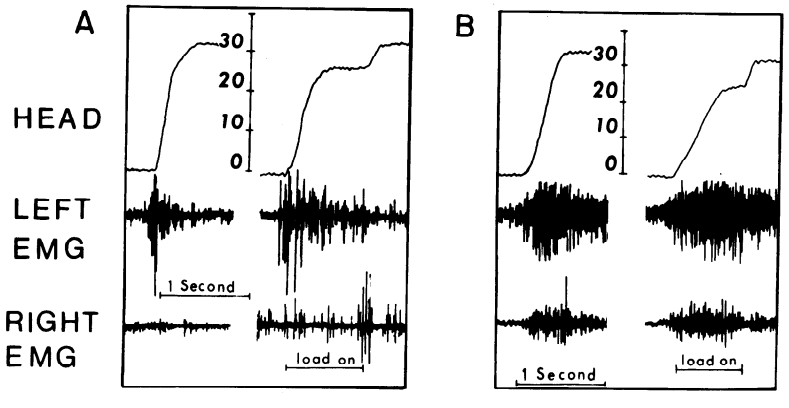

FIG. 5. Visually triggered head movements in chronically vestibulectomized monkey. *A*: preoperative. An unloaded head movement (left) is compared with loaded head movement (right), both movements are elicited by the appearance of a target, but performed in total darkness. Note the head returns to the same final position after removal of the load. EMG: electromyographic activity recorded from left and right splenii capitis. *B*: after dorsal root section (C_1–T_2). Note slowing down of loaded head movement and cocontraction. Both unloaded and loaded movements elicited by the appearance of target, but performed in total darkness.

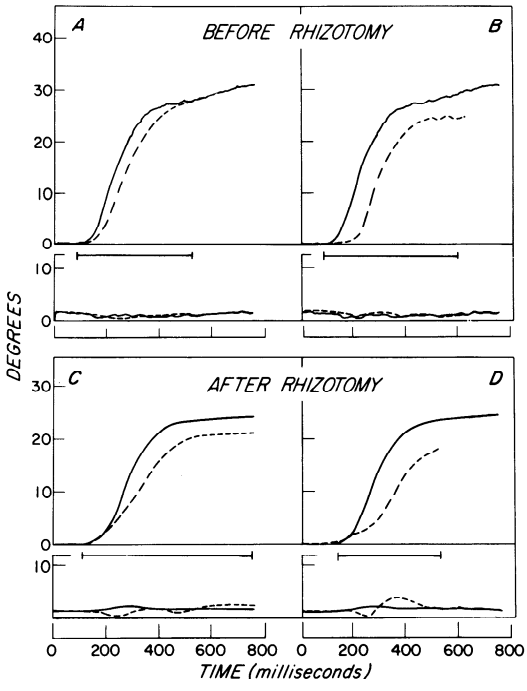

FIG. 6. Unloaded movements (solid lines) and movements loaded with a step of torque (dashed lines) are presented for the intact (*A* and *B*) and the rhizotomized animal (*C* and *D*). The effect of loads of two different magnitudes is indicated: a load of 0.035 Nm in the left part of the figure (*A* and *C*), and a load of 0.077 Nm in the right part of the figure (*B* and *D*). In each panel, the upper two curves represent the average of selected (4–10) unloaded movements. Since the duration of load application was between 400 and 800 ms, only the first 400 ms of load application is shown. The corresponding standard deviations are presented in the lower two curves.

movement. As shown in Fig. 5*A*, an unexpected application of a step of constant force at the beginning and for the duration of a head movement resulted in an increase in electromyographic activity (EMG) in the agonist muscles. This change in EMG activity was due to a change in the flow of proprioceptive afferent impulses from muscles, tendons, and perhaps joint receptors mediated by segmental and presumably suprasegmental circuits. (The animal was in total darkness during application of the load.) Loading the head during a movement was repeated a number of times in a random fashion in the course of a single experimental session. Averages of loaded and unloaded head-movement curves for one experimental session in which step torque loads of two different magnitudes were used are shown in Fig. 6*A* and *B*.

HEAD MOVEMENTS IN CHRONICALLY RHIZOTOMIZED MONKEYS. To evaluate the relative contribution of the neck reflex apparatus, we sectioned all the cervical and the upper thoracic dorsal roots (C_1–T_2). Following this surgical intervention, head movements could easily be elicited by target presentation from all three operated animals. As in the preoperative condition, target lights were used to trigger the eye-head response, but they were turned off just prior to the initiation of the head movement (leaving the room in complete darkness). Consequently, the head reached its intended position without any assistance from either visual, vestibular, or proprioceptive cues (Fig. 5*B*). When loads were *unexpectedly* applied to these animals, the head movements were found to be slower when compared to that of the same animal with intact proprioception (Fig. 5*A*). Figure 6*C* and *D* shows the averaged unloaded and loaded head movements for one experimental session in which step torque loads of two different magnitudes were randomly applied. The comparison of the preoperative differences between unloaded and loaded trajectories with the postoperative differences provided an estimate of the relative contribution of the proprioceptive apparatus. Figure 6*C* and *D* also indicates that the differences between loaded and unloaded movements after deafferentation were larger because only the mechanical properties of the neck musculature were left to provide for load compensation. Table 2 summarizes our computations on these averaged trajectories. The differences in the areas under the loaded and unloaded averaged curves were expressed as a percentage of the area under the unloaded curves. The comparison of these differences indicated that load compensation in our experimental conditions was rather modest.

TABLE 2. *Difference in areas under unloaded and loaded head-movement curves*

Monkey	Load, g·cm	Intact, % I	Rhizotomized, % R	Change After Rhizotomy, % R − I
M43	315	12 ± 5 (10)	36 ± 13 (10)	24
M50	357	60 ± 12 (9)	79 ± 11 (8)	19
M54	357	28 ± 8 (10)	37 ± 14 (12)	9
	789	49 ± 10 (9)	67 ± 18 (8)	18

Values are means ± SD. Numbers in parentheses are *n*. The area under each head-movement curve was measured over an interval of 140 ms after the application of the load. The difference in areas under the unloaded and loaded movement curves is expressed as a percentage of the area under the unloaded curve in order to account for changes in the unloaded head trajectory after rhizotomy. Each movement is an average of the results of a single day.

The examination of the postoperative pattern of neck muscle EMG activity showed the presence of some difference with the preoperative records (Fig. 5*A*). In fact, after dorsal root section, the agonist muscles usually achieved head turning by way of a sharp increase in activity which started before the movement, continued unmodified throughout it, and persisted while the head achieved the intended final position. In addition, cocontraction of agonist and antagonist muscles often occurred (Fig. 5*B*).

Because it is not known whether these postoperative changes should be taken as evidence of adaptive reorganization of motor programs or due to the loss of the reciprocal inhibition provided by the afferent pathways, there might be some question about relying exclusively on a direct comparison of pre- and postoperative head movements. Consequently, for our computation of the load-compensating capacities of the neck proprioceptive apparatus, we followed a different approach based on modeling and simulation.

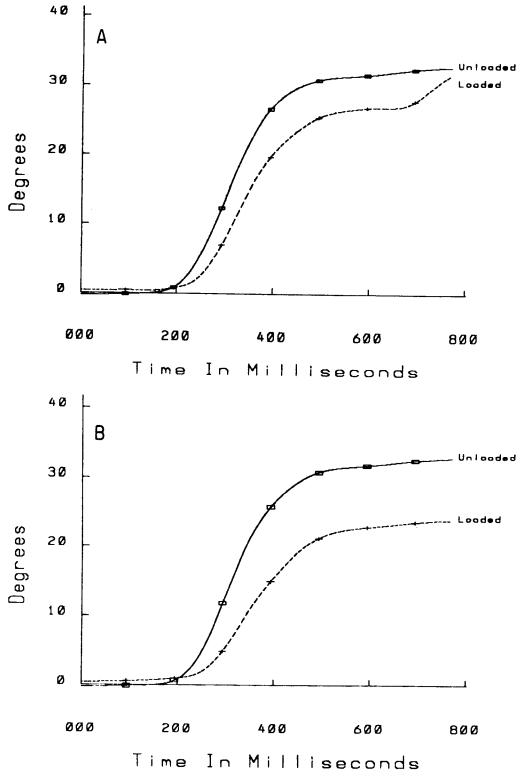

FIG. 7. Unloaded and loaded head movements generated by the monkey (*A*) are compared with simulated unloaded and loaded movements generated by the model (*B*). The simulated movements are generated in two steps. First, the input to the model is computed using *equation 1* and the unloaded monkey-generated movement. Next, this input is applied to the model to generate a simulated unloaded movement, using *equation 1* in reverse, or to generate a simulated loaded movement, using *equation 6*. The applied load is a step of torque of magnitude 0.035 Nm.

Contribution of reflex activity to load compensation: simulation of a model of head-neck system

To estimate the neural and mechanical contributions to load compensation, we used a computer simulation of the model developed above in which are represented the active and passive mechanical properties of the head-neck system (see METHODS section). The strategy was to use the model to predict the trajectory that the monkey's head would follow during a loaded movement if the feedback loop were inoperative and to compare this simulated loaded movement with the loaded movement actually generated by the intact animal. Any difference between these two movements was attributed to the effect of the reflex loop.

The crucial step in generating simulated head movements is the determination of the input or driving function. The significance of having estimated the values of the mechanical parameters of the model is that it allows us to compute this input. For a head movement, $\theta(t)$, obtained by averaging a set of unloaded monkey-generated movements, the corresponding input, $\mathrm{i}(t)$, is given by the equation

$$\mathrm{i} = \mathrm{I}\ddot{\theta} + (B_\mathrm{p} + B_\mathrm{a})\dot{\theta} + (K_\mathrm{p} + K_\mathrm{a})\theta \qquad (1)$$

Note that *equation 1* can also be used in the reverse direction, that is, for a known input function $\mathrm{i}(t)$, it is possible to compute a resulting head movement, $\theta(t)$. A movement so obtained will be termed a model-generated movement. Figure 7*A* illustrates an unloaded monkey-generated movement and a corresponding unloaded model-generated movement (Fig. 7*B*). By definition, the two are identical because the monkey-generated unloaded movement is used in *equation 1* to obtain an input, $\mathrm{i}(t)$, which is then reinserted in *equation 1* to generate a model movement, $\theta(t)$. Any differences between the two movements result solely from the problem of numerical solution of equations on the computer.

The input, $\mathrm{i}(t)$, obtained above, can also be used to generate a model loaded movement, $\theta_\mathrm{l}(t)$, using the equation

$$\mathrm{i} = \mathrm{I}\ddot{\theta}_\mathrm{l} + (B_\mathrm{p} + B_\mathrm{a})\dot{\theta}_\mathrm{l} + (K_\mathrm{p} + K_\mathrm{a})\dot{\theta}_\mathrm{l} + \mathrm{L} \qquad (6)$$

Figure 7*B* illustrates the model-generated loaded movement and Fig. 7*A*, a loaded movement generated by the intact animal. It can be noted that the model-generated loaded movement is slower than that generated by the monkey and it falls further short of the unloaded final position. The model, of course, has no neural feedback as indicated by the fact that the input, $\mathrm{i}(t)$, remains

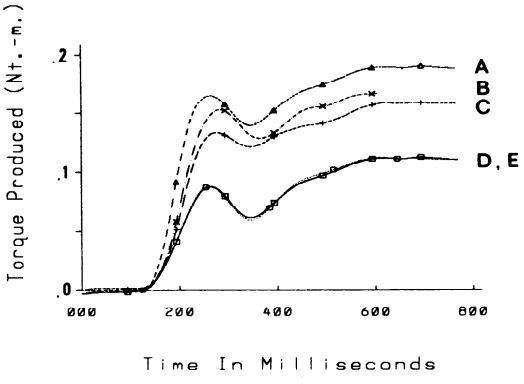

FIG. 8. The performance of the model (dashed lines) is compared to that of the intact monkey (solid lines) by computing torques required to generate movements under unloaded and loaded conditions. A, time course of torque necessary for either the monkey or the model to completely compensate for a load which is a step of torque of magnitude 0.035 Nm. B, torque developed by the monkey under the same loaded condition. (The line stops at the point where the load was removed.) C, torque developed by the model under the same condition. D, torque developed by the model when no load is applied. E, torque developed by the monkey when no load is applied. Marks on each line are spaced at 100-ms intervals.

unchanged when the load is applied. We, therefore, attribute the difference between the two loaded movements to the presence of neural feedback in the intact animal; however, the limitations of the model and the possible sources of errors are considered later.

In order to express quantitatively the effectiveness of the loop in units which are compatible with the applied load (a step of torque, rise time 50 ms), we computed the torque necessary to drive each of these movements. This is the torque which is developed by active muscle (*equation 5*) and which overcomes passive resistance to movement (*equation 4*). For unloaded movements, this torque is represented as

$$T = I\ddot{\theta} + B_p\dot{\theta} + K_p\theta \qquad (4)$$

and for loaded movements, it is

$$T = I\ddot{\theta}_1 + B_p\dot{\theta}_1 + K_p\theta_1 + L \qquad (7)$$

The torque represented in Fig. 8 illustrates the results of these computations. The main point of the figure is the difference between curves B and C where curve C represents the torque generated by the model when the load is applied (the model does not have any feedback) and curve B represents the torque which is generated by the intact animal. Both are computed using *equation 7* but using model-generated and monkey-generated loaded movements, respectively. The difference which is reported (Table 3) expresses the contribution of the feedback loops. We have expressed these differences as a percent of the torque necessary for full compensation which we computed and represented in curve A (curve A is the sum of curve D and the applied load, L). The purpose of showing curves D and E (*equation 4*) which represents torques required for unloaded model and monkey head movements is to display the extent of increase in torque due to the mechanical property of the musculature (indicated by the difference between curves C and D). We would like to emphasize that the difference between D and C is much larger than the difference between C and B; thus, indicating that the load compensation due to mechanical factors is larger than that due to neural feedback. Another aspect of Fig. 8 is the difference between curves A and B, which indicates that there is no perfect compensation. This conclusion may not

TABLE 3. *Mechanical and neural components of compensatory torque*

Monkey	Load, Nm	Increase in Torque, Nm		Compensation, %	
		Mechanical	Neural	Mechanical*	Neural†
43	0.0225	0.0040	0.0018	18	8
	0.0280	0.0051	0.0022	18	8
	0.0481	0.0095	0.0041	20	9
	0.0546	0.0093	0.0081	17	15
	0.0592	0.0102	0.0043	17	7
	0.0976	0.0197	0.0120	20	12
50	0.0278	0.0076	0.0022	27	8
	0.0278	0.0076	0.0032	27	12
54	0.0263	0.0093	0.0035	35	13
	0.0649	0.0289	0.211	45	33
	0.1008	0.0393	0.0297	39	29
	0.1013	0.0394	0.0323	39	32
	0.1023	0.0424	0.0316	41	31

* Lower bound. † Upper bound (see text for details).

apply for loads outside the range used here. Finally, we would like to comment on the fact that curves D and E are identical. This is because, as mentioned before, the underlying movements are, by definition, identical and, consequently, driven by identical torques.

In order to compute the simulated movements generated by the model (Fig. 7*B*), estimates of the temporal variation of active muscle properties, K_a and B_a, were required. These have not been directly measured in our system. However, in the model, we assume that they remained constant throughout the movement, with values of muscle stiffness corresponding to those most commonly found when the deafferented animal maintained a straight-ahead posture, with levels of EMG activity comparable with those observed in the preoperative state. These values are presented in Table 1 and they represent the lower end of the spectrum of values observed for K_a and B_a. As mentioned before, no significant dependence of B_a on EMG levels was observed. Increased neural input during movement is probably accompanied by an increase in the stiffness of the monkey's musculature. The consequence, in the model, of assuming a constant, low value of muscle stiffness, K_a, is that a "lower bound" is obtained for the magnitude of mechanically generated compensatory torque (difference between curves C and D, Fig. 8). Simultaneously, we obtain an "upper bound" for the reflexly induced compensatory torque (difference between curves B and C).

The difference between curves B and C is an estimated upper bound of the torque contributed by the reflex loop. For simplicity in tabular presentation of the results (Table 3), the difference in the curves B and C has been averaged over the first 200 ms after the application of a load disturbance and normalized with respect to the applied load (difference between curves A and D, averaged over the same 200-ms interval). It should be noted that there is a temporal variation in the difference of the two curves over time. However, it was beyond the scope of our experiments to analyze the cause underlying this variation, and we do not know whether to attribute it to activity of suprasegmental pathways or to nonlinearities in the mechanical parameters during a movement.

Figure 8 illustrates the application of the model to data which were collected in a single day and with a single kind of load. A similar analysis was carried out for loads of different sizes and for data obtained on different days for each of three monkeys. The results, indicated in Table 3, show that in the first 200 ms after the application of the disturbance, the upper bound of the contribution of reflex activity to load compensation is from 10 to 30% in different monkeys, as judged through simulation of a model of the head-neck system. In all cases, the contribution of mechanical components to load compensation was substantial (20–40%), always exceeding that of the neural component.

Because, undoubtedly, muscle stiffness increases with increased neural input to the muscle, we tested the effect of varying stiffness by computer simulation. The results indicated that a doubling of muscle stiffness during the movement would decrease our estimate of reflexly induced compensatory torque by 12%. Therefore, for two animals (*43* and *50*), simulated variation in muscle stiffness would completely account for all compensatory torque developed during a loaded movement. For the third animal, up to 20% of the compensatory torque would still be estimated to be of reflex origin.

Validation of the model was obtained by computing the torque developed during movements performed by a rhizotomized monkey and by comparing this result with that deduced from the model (Fig. 9). Since all relevant proprioceptive loops are absent in the rhizotomized animal, the torque that is developed during a loaded movement should be identical to that developed by the model, that is, the curve corresponding to curve B should be identical to curve C. A comparison showed that these curves were very similar (percentage of compensatory torque not attributable to mechanical factors was below 5% during the first 200 ms), and the performance is indicated in Table 4. The close similarity also

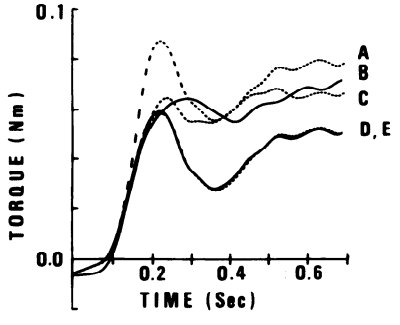

FIG. 9. The performance of the model (dashed lines) is compared to that of the deafferented monkey (solid lines) by computing torques required to generate movements under unloaded and loaded conditions. A, time course of torque necessary for either the monkey or the model to completely compensate for a load which is a step of torque of magnitude 0.07 Nm. B, torque developed by the monkey under the same loaded condition. C, torque developed by the model under the same condition. D, torque developed by the model when no load is applied. E, torque developed by the monkey when no load is applied.

TABLE 4. *Mechanical and neural components of compensatory torque: steps of torque applied to rhizotomized animals*

Monkey	Load, Nm	Increase in Torque, Nm		Compensation, %	
		Mechanical	Neural	Mechanical	Neural*
50	0.0261	0.0056	−0.0002	22	NS
54	0.0252	0.0089	−0.0009	35	NS
	0.0559	0.0195	0.0021	35	NS

NS, not significant. * Within the error limits of the model (i.e., below 5%).

indicated that any role of stiffness variation during movement was not a significant one in the rhizotomized animal.

DISCUSSION

Our studies were directed at evaluating quantitatively the effectiveness of the neck musculature when an unexpected load disturbance was applied during centrally initiated head movements. We approached this problem in two ways: first, by surgically interrupting the afferent loop subserving the reflex action and second, by building a mathematical model of the head-neck system and going through a process of simulation. Both methods provided roughly similar answers and showed that during the first 200 ms, the contribution of the neural component relative to the applied disturbance ranged from 10 to 30% of full compensation in different animals and that a significant portion (from 20 to 40%) of the total compensation was due to the intrinsic mechanical properties of the musculature. However, the combined reflex and mechanical torque never did provide a full compensation.

In a sense these results are not entirely surprising. In fact, the computations of Vallbo (38) on the basis of results from human subjects, Grillner's (18) experiments with decerebrate cats, and Allum's (1) results on postural resetting had already suggested that reflex load compensation was rather modest. Furthermore, there are a priori reasons to believe that animals are not "at the mercy of an invariantly stiff servo" as pointed out by Matthews (27) and Lundberg (24). However, our results represent the first evaluation of the effectiveness of load compensation during centrally generated movements.

We obtained evidence on the load-compensating capacities of both the neck musculature and the reflex apparatus, not only by sectioning the fibers subserving the reflex action, but also by using a method based on modeling the neck-head system. Knowledge of the mechanical properties of passive tissue permitted us to estimate the total compensatory torque developed during the application of a step torque load. To subdivide this into reflex and mechanical components required a knowledge of the active muscle stiffness during movement. Because increased neural output is generally correlated with increased muscle stiffness (1, 2, 20, 33), the burst of neural activity during a movement is probably accompanied by an increase in stiffness. An assumption of a constant stiffness, having a value equal to that of the mean stiffness during a forward-facing posture, results in an estimate of the neural contribution of the reflex loop as ranging from 10 to 30% in different monkeys. Any increase of muscle stiffness during a movement can only reduce this estimate. Thus, we obtain an upper limit to the contribution of the reflex loop to load compensation.

A major assumption in the model is that the head-neck system can indeed be well represented as a lumped second-order system. The model used is the simplest possible representation of a mechanical system with inertial, viscous, and elastic properties, where the input does not act directly on these passive components but acts through a viscoelastic element, thus taking into account the length-tension and force-velocity properties of muscle. While it is acknowledged that the mechanical characteristics of muscle and other tissue are nonlinear, no attempt was made to develop a more detailed model of muscle or of other tissue primarily because the measurements were not available to differentiate between various possible models.

Given these assumptions, it is relevant to consider here, whether the model we have devised is strictly ad hoc or whether it represents a tool able to handle head-movement data collected under different conditions. Our controls have been addressed to this question and we have shown that the model can correctly predict the trajectory of inertially loaded or step torque-loaded movements of deafferented animals. Furthermore, the model was utilized with conservatively chosen, low values of muscle stiffness such as occurred during postural situations with low levels of electromyographic activity. Accordingly, we believe that the results derived from modeling taken together with those ob-

tained after dorsal root section correctly indicate the upper limit of the reflex load compensation.

We have also shown that under certain circumstances, in particular if a doubling of active muscle stiffness occurs during movement, no reflex load compensation is necessary to account for the observed loaded movements. Values of muscle stiffness greater than double the value utilized in the model have been observed in postural situations.

While our experiments represent an evaluation as to just how much reflex torque can be generated by the neck muscle when an opposing load was applied, we feel that the following qualification should be added for their correct interpretation. First of all, it should be made clear that our animals had no special incentive or reason to overcome the unexpected load during head movements. Our monkeys were not trained to move their heads to a certain position, but chose to program a head movement together with an eye movement in order to perform the discrimination task (6). Although the actual movement of the head occurs after the saccadic eye movement, electromyographic recordings from eye and neck muscles indicated that the neural commands are delivered first to all neck muscles and then to those of the eyes (5). Consequently, these head movements are preprogrammed and are not the result of the particular paradigm employed in our experiments.

It is perhaps important to emphasize that the sudden and unexpected application of a load opposing the head movement, while producing head slowing and undershoot, did not basically prevent the animal from obtaining the reward. In fact, only after the target light, which was turned off during eye-head movement, reappeared, was the animal able to make the visual discrimination necessary to acquire the reward. In this way we were able to observe the consequences of load application uncomplicated by early reprogramming. This particular experimental strategy happened to be optimal from our standpoint because we intended to measure the reflex proprioceptive capabilities in normal, "ordinary" movements, unexpectedly met by an external disturbance. It should be pointed out that while we do not know the level of alpha-gamma coactivation during head movements, we have always observed clear-cut, short-latency reflex proprioceptive responses in the neck electromyogram following the application of a load disturbance. These electromyographic patterns were qualitatively similar to those that have been observed in other somatic muscles. It is interesting that in contrast to the reflex properties of the neck muscles, the motoneurons innervating the eye muscles have been shown to be insensitive to large externally applied disturbances (21). Naturally, it will remain for future experimentation to inquire whether the gain of the reflex proprioceptive apparatus can be significantly changed in other, more demanding tasks or when different and more specific instructions are given to the animal.

It could be argued that the values of reflex torque observed in our experimental conditions might be due to the fact that we have dealt with the neck muscles which, while richly endowed with muscle spindles (10), might not under ordinary circumstances be subjected to external changes in load. However, this is unlikely because, on the basis of simple mechanical considerations, it is evident that the torque applied to the neck muscles changes every time there is relative motion of the head on the trunk. Moreover, one can think of many circumstances when monkeys use their neck muscles to meet external disturbances—the pursuit of food and fighting being examples.

A third qualification pertains to the fact that the loads which impeded movement were relatively large. Assuming that the spindle afferents in neck muscles have high sensitivity for small disturbances, but "saturate" relatively easily, one might expect that the reflex component of load compensation will be greater for small load disturbances than for large load disturbances.

Finally, although there is little doubt that the proprioceptive apparatus generates a certain amount of torque to overcome an external disturbance, the question still remains whether load compensation is the only major function for this apparatus. For example, it could be argued that the neck proprioceptive apparatus might subserve some of the synergistic cocontraction that must occur when head rotations are made from body positions which are off the vertical. Although we have not investigated this possibility, the cocontraction, which was observed after bilateral deafferentation, might well be an adaptive response to the loss of afferent proprioceptive input. Another alternative, based on observing the behavior of stretched and released muscles in decerebrate preparations with or without afferent feedback, indicates in the proprioceptive apparatus an important source of signals necessary for linearizing muscle properties (11, 30). Recently the importance of proprioceptive signals in the adaptive modification of central programs through a process of gain changes as well as changes in the coupling among active muscles has been stressed (29).

Our conclusions and the latter hypotheses need not be seen as mutually exclusive. Given the widespread segmental and suprasegmental distribution of afferent proprioceptive signals, it is entirely possible that short latency but modest load compensation represents the first line of

defense against an opposing load before the intervention of longer latency adaptive modifications.

ACKNOWLEDGMENTS

We thank Drs. J. H. J. Allum and J. Houk for reading the manuscript and T. Heyward for typing it.

This project was supported by National Institute of Neurological Diseases and Stroke Research Grant NS09343, and National Aeronautics and Space Administration Grant NGR 22-009-798.

Present address of P. Morasso: Istituto di Elettrotecnica, Viale Causa 13, 16145 Genova, Italy.

REFERENCES

1. ALLUM, J. H. J. Responses to load disturbances in human shoulder muscles: the hypothesis that one component is a pulse test information signal. *Exptl. Brain Res.* 22: 307–326, 1975.
2. BARMACK, N. H. Measurements of stiffness of extraocular muscles of the rabbit. *J. Neurophysiol.* 39: 1009–1019, 1976.
3. BERTHOZ, A. Afferent neck projection to the cat cerebellar cortex. *Exptl. Brain Res.* 20: 385–401, 1974.
4. BIZZI, E. The coordination of eye-head movements. *Sci. Am.* 231: 100–106, 1974.
5. BIZZI, E., KALIL, R. E., AND TAGLIASCO, V. Eye-head coordination in monkeys: evidence for centrally patterned organization. *Science* 173: 452–454, 1971.
6. BIZZI, E., POLIT, A., AND MORASSO, P. Mechanisms underlying achievement of final head position. *J. Neurophysiol.* 39: 435–444, 1976.
7. BROOKS, V. B., HORE, J., MEYER-LOHMANN, J., AND VILIS, T. Cerebellar pathway for precentral responses following arm perturbations. *Neurosci. Abstr.* 2: 516. 1976.
8. CLIFTON, G. L., VANCE, W. H., APPELBAUM, M. L., COGGESHALL, R. E., AND WILLIS, W. D. Responses of unmyelinated afferents in the mammalian ventral root. *Brain Res.* 82: 163–167, 1974.
9. CONRAD, B., MATSUNAMI, C., MEYER-LOHMANN, J., WIESENDANGER, M., AND BROOKS, V. B. Cortical load compensation during voluntary elbow movements. *Brain Res.* 81: 507–514, 1974.
10. COOPER, S. AND DANIEL, P. M. Muscle spindles in man: their morphology in the lumbricals and the deep muscles of the neck. *Brain* 86: 563–586, 1963.
11. CRAGO, P. E., HOUK, J. C., AND HAZAN, Z. Regulatory action of human stretch reflex. *J. Neurophysiol.* 39: 925–935, 1976.
12. DAVIS, J. N. AND SEARS, T. A. The proprioceptive reflex control of the intercostal muscles during their voluntary activation. *J. Physiol., London* 209: 711–738, 1970.
13. DICHGANS, J., BIZZI, E., MORASSO, P., AND TAGLIASCO, V. Mechanisms underlying recovery of eye-head coordination following bilateral labyrinthectomy in monkeys. *Exptl. Brain Res.* 18: 548–562, 1973.
14. EVARTS, E. V. A technique for recording activity of subcortical neurons in moving animals. *Electroencephalog. Clin. Neurophysiol.* 24: 83–86, 1968.
15. EVARTS, E. V. Motor cortex reflexes associated with learned movement. *Science* 179: 501–503, 1973.
16. EVARTS, E. V. AND TANJI, J. Reflex and intended responses in motor pyramidal tract neurons of monkey. *J. Neurophysiol.* 39: 1069–1080, 1976.
17. GRANIT, R., HOLMGREN, B., AND MERTON, P. A. The two routes for excitation of muscle and their subservience to the cerebellum. *J. Physiol., London* 130: 213–224, 1955.
18. GRILLNER, S. The role of muscle stiffness in meeting the changing postural and locomotor requirements for force development of the ankle extensors. *Acta Physiol. Scand.* 86: 92–108, 1972.
19. HAMMOND, P. H. An experimental study of servo action in human muscular control. *Intern. Congr. Med. Electron., 3rd, London, 1960,* p. 190–199.
20. HOUK, J. C., SINGER, J. J., AND GOLDMAN, M. R. An evaluation of length and force feedback to soleus muscle of decerebrate cats. *J. Neurophysiol.* 33: 784–811, 1970.
21. KELLER, E. L. AND ROBINSON, D. A. Absence of a stretch reflex in extraocular muscles of the monkey. *J. Neurophysiol.* 34: 908–919, 1971.
22. LAMARRE, Y. AND LUND, J. P. Load compensation in human masseter muscles. *J. Physiol., London* 253: 21–35, 1975.
23. LUCIER, G. E., RÜEGG, D. C., AND WIESENDANGER, M. Responses of neurons in motor cortex and in area 3a to controlled stretches of forelimb muscles in the cebus monkeys. *J. Physiol., London* 251: 833–853, 1975.
24. LUNDBERG, A. Reflex control of stepping. *Nansen Memorial Lecture.* Oslo: Universitetforlaget, 1969, p. 42.
25. MARSDEN, C. D., MERTON, P. A., AND MORTON, H. B. Servo action in the human thumb. *J. Physiol., London* 257: 1–44, 1976.
26. MARSDEN, C. D., MERTON, P. A., AND MORTON, H. B. Stretch reflexes and servo actions in a variety of human muscles. *J. Physiol., London* 259: 531–560, 1976.
27. MATTHEWS, P. B. C. *Mammalian Muscle Receptors and Their Central Actions.* Baltimore: Williams & Wilkins, 1972.
28. MURPHY, J. T., WONG, Y. C., AND KWAN, H. C. Afferent-efferent linkages in motor cortex for single forelimb muscles. *J. Neurophysiol.* 38: 990–1014, 1975.
29. NASHNER, L. M. Adapting reflexes controlling the human posture. *Exptl. Brain Res.* 26: 59–72, 1976.
30. NICHOLS, T. R. AND HOUK, J. C. The improvement in linearity and the regulation of stiffness that results from the actions of the stretch reflex. *J. Neurophysiol.* 39: 119–142, 1976.
31. PHILLIPS, C. G. The motor apparatus of the baboon's hand. *Proc. Roy. Soc., London, Ser. B* 173: 141–174, 1969.

32. PHILLIPS, C. G., POWELL, T. P. S., AND WIESENDANGER, M. Projections from low-threshold muscle afferents of hand and forearm to area 3a of baboon's cortex. *J. Physiol., London* 217: 419–444, 1971.

33. RACK, P. M. H. AND WESTBURY, D. R. The effects of length and stimulus rate on tension in the isometric cat soleus muscle. *J. Physiol., London* 204: 443–460, 1969.

34. SEARS, T. A. Efferent discharges in alpha and fusimotor fibers of intercostal nerves of the cat. *J. Physiol., London* 174: 295–315, 1964.

35. SEVERIN, F. V., ORLOVSKY, G. N., AND SHIK, M. L. Work of the muscle receptors during controlled locomotion. *Biophysics, USSR* 12: 575–586, 1967.

36. TAYLOR, A. AND CODY, F. W. J. Jaw muscle spindle activity in the cat during normal movements of eating and drinking. *Brain Res.* 71: 523–530, 1974.

37. VALLBO, Å. B. Slowly adapting muscle receptors in man. *Acta Physiol. Scand.* 78: 315–333, 1970.

38. VALLBO, Å. B. The significance of intramuscular receptors in load compensation during voluntary contractions in man. In: *Control of Posture and Locomotion*, edited by R. B. Stein, K. G. Pearson, R. S. Smith, and J. B. Redford. New York: Plenum, 1973, p. 211–226.

39. VON EULER, C. Proprioception control and respiration. In: *Nobel Symposium I; Muscular Afferents and Motor Control*, edited by R. Granit. Stockholm: Almquist & Wilksell, 1966, p. 197–207.

40. WIESENDANGER, M. Input from muscle and cutaneous nerves of the hand and forearm to neurones of the precentral gyrus of baboons and monkeys. *J. Physiol., London* 228: 203–219, 1973.

41. YUMIYA, H., KUBOTA, K., AND ASANUMA, H. Activities of neurons in area 3a of the cerebral cortex during voluntary movements in the monkey. *Brain Res.* 78: 169–176, 1974.